PROTEINS: Structure, Function, and Genetics 51:137–146 (2003)

Characterization of the Electrophile Binding Site and Substrate Binding Mode of the 26-kDa Glutathione S-Transferase from *Schistosoma Japonicum*

Rosa M.F. Cardoso,[1,2] Douglas S. Daniels,[1] Christopher M. Bruns,[3] and John A. Tainer[1]*
[1]*Skaggs Institute for Chemical Biology, The Scripps Research Institute, La Jolla, California*
[2]*Grupo de Cristalografia de Proteínas, Institutos de Física e Química de São Carlos, Universidade de São Paulo, São Carlos, São Paulo, Brazil*
[3]*Incyte Genomics, Palo Alto, California*

ABSTRACT **The 26-kDa glutathione S-transferase from *Schistosoma japonicum* (Sj26GST), a helminth worm that causes schistosomiasis, catalyzes the conjugation of glutathione with toxic secondary products of membrane lipid peroxidation. Crystal structures of Sj26GST in complex with glutathione sulfonate (Sj26GSTSLF), S-hexyl glutathione (Sj26GSTHEX), and S-2-iodobenzyl glutathione (Sj26GSTIBZ) allow characterization of the electrophile binding site (H site) of Sj26GST. The S-hexyl and S-2-iodobenzyl moieties of these product analogs bind in a pocket defined by side-chains from the β1-α1 loop (Tyr7, Trp8, Ile10, Gly12, Leu13), helix α4 (Arg103, Tyr104, Ser107, Tyr111), and the C-terminal coil (Gln204, Gly205, Trp206, Gln207). Changes in the Ser107 and Gln204 dihedral angles make the H site more hydrophobic in the Sj26GSTHEX complex relative to the ligand-free structure. These structures, together with docking studies, indicate a possible binding mode of Sj26GST to its physiologic substrates 4-hydroxynon-2-enal (4HNE), *trans*-non-2-enal (NE), and ethacrynic acid (EA). In this binding mode, hydrogen bonds of Tyr111 and Gln207 to the carbonyl oxygen atoms of 4HNE, NE, and EA could orient the substrates and enhance their electrophilicity to promote conjugation with glutathione. Proteins 2003;51:137–146.**
© 2003 Wiley-Liss, Inc.

Key words: glutathione S-transferase; *Schistosoma japonicum;* lipid peroxidation; 4-hydroxynon-enal; ethacrynic acid; docking; schistosomiasis

INTRODUCTION

Glutathione S-transferases (GSTs) are a family of multifunctional isoenzymes involved in the neutralization of potentially toxic compounds, cellular mechanism of drug resistance, biosynthesis of leukotrienes, and intracellular binding and transport of hydrophobic ligands.[1] Most of these functions rely on catalysis of the nucleophilic addition of glutathione (γ-Glu-Cys-Gly) to a wide variety of electrophiles by GSTs.[1,2] Glutathione conjugates have greater solubility in water and are easily exported from the cell, where they are metabolized via the mercapturate pathway and are eventually excreted. In addition, GSTs bind a range of neutral or anionic lipophilic chemicals that are not substrates, including steroid and thyroid hormones, bilirubin, and heme. Binding of these nonsubstrate compounds may not only contribute to their transport and elimination but also create a bound reserve of hormones in target organs, minimizing the effects of transient fluxes.[1]

GSTs from a variety of organisms have been identified and characterized. Cytosolic GSTs have been grouped into seven major species-independent classes (alpha, mu, omega, pi, sigma, theta, and zeta) on the basis of their differing biochemical and immunologic properties and amino acid sequence.[2,3] In general, the sequence identity within a class is high (about 70%) whereas the identity between the classes is much lower (typically less than 30%). Representative crystal structures from each cytosolic class have been determined[3–11] and reveal that cytosolic GSTs are hetero- or homodimers with a common 3D fold. Each subunit contains two domains: an N-terminal α/β domain, which binds to glutathione in a conserved mode throughout the classes, and an α-helical C-terminal domain, which predominantly composes the substrate binding site and is less well conserved at the sequence and structural levels, with the helices varying in number, length, curvature, and orientation.[2] Adjacent binding sites for glutathione (the "G" site) and the electrophilic substrates (the "H," or hydrophobic, site) promote the glutathione conjugation reaction. Further, dimerization appears to be essential for maintaining thermodynamically stable and functional GST structures.[12]

GSTs have also been detected in a range of pathogenic helminths, likely comprising a major detoxification pathway and a primary defense against oxidative damage.[13] Two GST isoenzymes, of 26 and 28 kDa, are found in *Schistosoma japonicum*,[14] a helminth worm that causes schistosomiasis, which is the second most common parasitic disease in the world and affects 200 million people. The structure of the 26-kDa GST from *S. japonicum* was

*Correspondence to: John A. Tainer, Skaggs Institute for Chemical Biology, The Scripps Research Institute, MB-4, 10550 N. Torrey Pines Rd., La Jolla, CA 92037. E-mail: jat@scripps.edu

Received 12 August 2002; Accepted 4 November 2002

© 2003 WILEY-LISS, INC.

solved independently by two groups.[15,16] As in other GSTs, the 218 residues of each subunit of the Sj26GST dimer form a small N-terminal α/β domain (residues 1–76), a shorter linker region (residues 77–84), and a larger α-helical C-terminal domain (residues 85–218).[15,16] The Sj26GST dimer assembly creates a long (40 Å) and narrow (approximately 6–10 Å) interdomain cleft.[15] The sequence and structural homology of Sj26GST are most similar to the mu class, although it exhibits a mixture of alpha-, mu-, and pi-type biochemical characteristics.[14]

Two main functions of Sj26GST are conjugation of glutathione to carbonyl-containing secondary products of lipid peroxidation and solubilization of heme resulting from metabolism of host erythrocytes. Both functions are likely crucial to the worm's survival as free-radical-induced damage or a buildup of insoluble heme within the parasite would be lethal. Indeed, induction of antibodies capable of inhibiting SjGST activity results in significant protection against schistosomiasis, offering a possible vaccination strategy.[17–20] Established secondary products of membrane lipid peroxidation recognized by Sj26GST include *trans,trans*-alkadienals, *trans*-alkenals, and 4-hydroxyalkenals.[14] The major 4-hydroxyalkenal formed during peroxidation of arachidonic and linoleic acids, 4-hydroxynon-2-enal (4HNE), is a particularly cytotoxic and mutagenic electrophile. At low levels, 4HNE also appears to be involved in cell cycle control and signal transduction.[21] Therefore, 4HNE intracellular concentration is tightly regulated, and the major metabolic pathway for 4HNE disposition is believed to be glutathione conjugation.[22] Sj26GST also shows high activity toward ethacrynic acid, which in vivo enhances excretion of sodium, chloride, and potassium with diuretic effects.[23] Sj26GST has also been shown to bind to therapeutic concentrations of praziquantel, the leading antischistosomal drug, in a nonsubstrate site at the dimer interface.[15] Therefore, GST not only mediates xenobiotic metabolism in *Schistosoma* but also affects drug–parasite interactions, contributing to the worm's drug resistance process and making Sj26GST an attractive drug target.

The variation in ligand recognition by GSTs from different organisms and classes is presumably due to differences in their H sites. To characterize the H site and gain insights into the diversity of substrates recognized by Sj26GST, we report here the crystal structures of Sj26GST in complex with the product analogs glutathione sulfonate (Sj26GSTSLF), S-hexyl glutathione (Sj26GSTHEX), and S-2-iodobenzyl glutathione (Sj26GSTIBZ). This is the first report of the structure of a helminth GST with a ligand occupying the H site. To promote general understanding of the binding of its physiological substrates, we also detail the computational docking of NE, 4HNE, and EA to Sj26GST.

MATERIALS AND METHODS

Expression, Purification, Crystallization, and Data Collection

Sj26GST was expressed as a recombinant product of the PGEX-3X expression vector (Amersham Pharmacia, Piscataway, NJ) and purified without the use of a glutathione affinity column as previously described.[24] Crystals of Sj26GST were grown at room temperature by hanging drop vapor diffusion against 48–50% saturated ammonium sulfate, 2% (v/v) ethanol, and 225 mM sodium acetate, pH 5.6, with dithiothrietol 10 mM and threalose 10 mM added to the mother liquor.[24] Crystals of Sj26GST in complex with glutathione sulfonate and S-2-iodobenzyl glutathione were obtained by cocrystallization after overnight preincubation of the ligand with Sj26GST in a molar ratio of 1:10 (protein:ligand) for Sj26GSTSLF and 1:5 for Sj26GSTIBZ complex. Crystals of Sj26GST in complex with S-hexyl glutathione were obtained by soaking the ligand-free Sj26GST crystals in the reservoir solution supplemented with 3 mM S-hexyl glutathione for 3 h before flash-freezing. Prior to being cooled to cryogenic temperatures, crystals were soaked in a cryoprotectant solution of mother liquor containing 20% (v/v) glycerol.

X-ray diffraction data for Sj26GSTSLF and Sj26GSTHEX complexes were collected on beamline 7-1 at the Stanford Synchrotron Radiation Laboratory using a MAR image plate and a liquid nitrogen cryostream maintained at 90 K. Data for Sj26GSTIBZ were collected on beamline A1 at the Cornell High Energy Synchrotron Source using a CCD detector and a liquid nitrogen cryostream maintained at 90 K. The data set of each complex was processed using the HKL package[25] and the CCP4 suite of programs.[26]

Structure Determination and Refinement

The structures of the Sj26GSTSLF, Sj26GSTHEX, and Sj26GSTIBZ complexes were solved by molecular replacement using AmoRe[27] and the ligand-free Sj26GST structure [Protein Data Bank (PDB) entry 1GTA][15] as a probe. Refinement of the Sj26GST complex structures was conducted with TNT[28] and CNS[29] using the maximum likelihood target function, bulk solvent, and anisotropic temperature factor corrections. R_{free} was calculated using the same set of randomly assigned reflections in both programs. Topology and parameter files for glutathione sulfonate and S-3-iodobenzyl glutathione were obtained from the Heterocompound Information Center-Uppsala (HIC-Up web server at http://xray.bmc.uu.se/hicup) and manually edited for S-hexyl glutathione and S-2-iodobenzyl glutathione. The refinement of the models proceeded through cycles of positional, temperature factor, and manual rebuilding in XFIT[30] into σA-weighted $2Fo - Fc$ and $Fo - Fc$ electron density omit maps. Water molecules were added manually and stereochemical analysis of the refined structures performed using PROCHECK.[31]

Structural Analysis

Structural changes between the ligand-free Sj26GST and Sj26GSTSLF, Sj26GSTHEX, Sj26GSTIBZ, and Sj26GST fused with a GP41 peptide and bound to glutathione (Sj26GSTGSH; PDB entry 1GNE)[16] were analyzed by superposition, visual inspection, and calculation of interdimer angles. Superpositions and root mean square (RMS) calculations were conducted using the INSIGHT II package (Accelrys Inc., San Diego, CA) for the pairs of superpositions between the ligand-free monomers and the four ligand-bound Sj26GST monomers using only the C_α atoms of α-helices and β-strands residues 12–34, 56–60, 68–78, 87–106,116–136, 150–184, and 188–193. As the crystallographic asymmetrical unit contains only one monomer, the

dimeric structures of the ligand-free Sj26GST, Sj26GSTSLF, Sj26GSTHEX, and Sj26GSTIBZ complexes were generated by creating the appropriate symmetry mate using PDBSET.[26] The difference in orientation between the subunits of the ligand-free and the four ligand-bound Sj26GST dimers was calculated by superposing one monomer of each dimer and determining the rotation matrix required to superimpose the second monomer. Hydrogen bonds were identified using HBPLUS.[32] Comparison to other GSTs involved superposition, as described above, with human GST M1-1 (PDB entry 1GTU), human GST M2-2 (2GTU), rat GST M1-1 (5FWG), and human GST A4-4 (1GUM).

Docking Simulations of the Physiologic Substrates Binding

To model Sj26GST interaction with the physiologic substrates *trans*-non-2-enal, 4-hydroxynon-2-enal, and ethacrynic acid, docking experiments were performed in AutoDock 3.05 using the Lamarckian Genetic Algorithm.[33] To mimic a nonconjugated glutathione-containing complex, we used the dimeric structure of Sj26GSTSLF, with water molecules and the glutathione sulfonate moiety removed. Polar hydrogen atoms were added to the protein and glutathione using Insight II and partial charges were assigned using PDB2PDBQ (from J.L. Pellequer, The Scripps Research Institute, La Jolla, CA) with the Amber force field.[34] AutoGrid chemical affinity and electrostatics maps were precalculated and centered on the C_β of the catalytic Tyr7 with 62 × 70 × 70 grid points at a spacing of 0.3 Å.

The ligand structures were generated using the Builder module of Insight II. Assignment of ligand partial charges and energy minimization were performed using the CVFF force field[35] and the Discovery 3 module for 100 interactions. This short minimization was enough to relieve any close contacts. The CH, CH2, and CH3 groups of the ligands were treated as united atoms by adjusting van der Waals parameters and partial atomic charges suitably. The s-*cis* and s-*trans* isomers of non-2-enal and 4-hydroxynon-2-enal were docked in the edited Sj26GSTSLF complex. However, because s-*trans* is the thermodynamically favorable species only those dockings are presented. During the docking simulations, torsion angles of all conjugated double bonds in each ligand were kept fixed. All other rotatable torsions were allowed to vary to confer ligand flexibility. No protein or glutathione atoms were allowed to move during the simulation. As a test of the method, glutathione sulfonate, S-hexyl glutathione, and S-2-iodobenzyl glutathione were docked into the Sj26GSTSLF complex (with ligand removed) and compared to the Sj26GSTSLF, Sj26GSTHEX, and Sj26GSTIBZ crystallographic complexes. AutoGrid maps for these test cases were centered between the G and H sites, with 55 × 50 × 60 grid points at a spacing of 0.375 Å.

Each ligand docking was limited to 256 runs, containing a maximum of 250,000 energy evaluations and 27,000 generations. Following docking, structures were sorted by total energy of interaction and sequentially assigned to cluster families with RMS deviation lower than 2 Å. Cluster analysis was performed in XFIT[30] and docking results were compared to the crystallographic complexes.

RESULTS AND DISCUSSION

Overall Comparison of the Sj26GST Structures

The structures of Sj26GST in complex with glutathione sulfonate, S-hexyl glutathione, and S-2-iodobenzyl glutathione were determined to characterize the electrophile binding site of Sj26GST. All three complexes are in the space group $P6_322$ with one subunit and one ligand per asymmetrical unit (Table I). The structure of the Sj26GSTHEX complex was refined to a resolution of 2.1 Å, R = 20.0%, and Rfree = 22.4%, Sj26GSTSLF to 2.3 Å, R = 21.8%, and Rfree = 26.1%, and Sj26GSTIBZ to 2.6 Å, R = 23.1%, and Rfree = 27.5% (Table I). The final models include all residues of Sj26GST except the two C-terminal residues (amino acids Pro217 and Lys218), for which definitive electron density was not observed. Omit maps clearly define the locations and conformations of the ligands in the binding site (Fig. 1).

The three structures have good geometry and the only residue present in the generously allowed region of the Ramachandran plot is Gln67 (mean ϕ and ψ for the three complexes are 85.4 ± 2.4° and 102.1 ± 2.3°, respectively), which has excellent electron density and is located in the glutathione binding site. The high energy of Gln67 is thought to be an important feature of binding to glutathione and has been observed as an outlier in the Ramachandran plot of other GST structures.[7,16] In addition, Pro56, located at the beginning of a β-strand, and Pro202, located in the C-terminal coil, adopt a *cis* peptide conformation in all three complexes, and this feature is also common to other GSTs.[7,16]

Dimers were generated to examine structural differences between the three complexes and the ligand-free Sj26GST.[15] The use of the dimeric structure was necessary to compose the G site. There are no large differences in the overall fold of the complexes and the ligand-free monomers [Fig. 2(A)], which have a C_α RMS deviation of 0.3 Å. However, the angle between monomers differs in each dimeric structure, with the complex dimers being 4.0–4.8° more open than the ligand-free dimer [Fig. 2(A)].

Glutathione Binding Site (G Site)

The conformation of the glutathione moiety in the Sj26GSTSLF, Sj26GSTHEX, and Sj26GSTIBZ complexes is nearly identical [Fig. 2(B)]. Each of the three residues comprising the glutathione moiety, γ-Glu-Cys-Gly, makes specific contacts with Sj26GST [Figs. 1 and 2(B)], mainly through hydrogen bonds. The glycyl carboxylate group of glutathione forms hydrogen bonds with the side-chains of Trp41 and Lys45 and the glycyl amino group forms a hydrogen bond with Asn54. The cysteinyl carbonyl forms a hydrogen bond with the side-chain of Trp8, while its amino moiety forms hydrogen bonds with the main-chain of Asn54 and Leu55. The sulfur atom of glutathione, the site of chemical conjugation with the electrophile, is about 3.2 Å away from the OH group of Tyr7, which is believed to activate the glutathione thiol group for the conjugation reaction.[1,2] Most of the interactions between Sj26GST and the glutathione moiety of the three ligands are located in the γ-glutamyl region. The γ-glutamyl amino group forms hydrogen bonds with the side-chain of Asp101 and Gln67, which adopts unusual main-chain dihedral angles. Gln67

TABLE I. X-Ray Diffraction Data and Model Statistics for Sj26GSTHEX, Sj26GSTHEX, and Sj26GSTHEX Complexes

	Sj26GSTHEX	Sj26GSTSLF	Sj26GSTIBZ
Crystal features			
Space group	$P6_322$	$P6_322$	$P6_322$
No. of monomers per asymmetrical unit	1	1	1
Matthews coefficient ($Å^3$ Da^{-1})	2.87	2.88	2.97
Solvent content (%)	56.85	56.95	58.31
Unit cell parameters (Å)	a=b: 114.9; c: 78.4	a=b: 115.1; c:78.3	a=b: 116.6; c: 78.8
Data quality			
Resolution (Å)[a]	27.9 - 2.1 (2.18–2.10)	26.0 - 2.3 (2.38–2.30)	26.0 - 2.6 (2.69–2.60)
No. of observations	80,211	137,582	56,234
No. of unique reflections	17,330	14,209	9,743
Mosaicity	0.43	0.72	0.23
Completeness (%)[a]	94.4 (63.4)	99.1 (93.2)	96.2 (89.4)
Multiplicity[a]	4.6 (3.6)	9.7 (8.1)	5.8 (4.6)
$I > 3\sigma(I)$ (%)[a]	73.4 (41.0)	76.2 (43.2)	76.3 (37.0)
R_{sym} (%)[a,b]	6.2 (29.6)	9.7 (57.8)	7.8 (68.9)
Model quality			
R (%)[c]	20.0	21.8	23.1
R_{free} (%)[d]	22.4 (5)	26.1 (10)	27.5 (10)
No. of residues	216	216	216
No. of water molecules	174	118	68
No. of ligands	1 S-hexyl-GSH	1 GSH sulfonate	1 S-2-iodobenzyl-GSH
Average B factor ($Å^2$)			
Protein overall	28.1	34.0	44.4
Protein main-chain	29.3	35.2	45.0
Ligand	26.6	41.4	59.4
Water molecules	40.4	43.2	43.4
RMS deviations			
Bond lengths (Å)	0.007	0.008	0.007
Bond angles (°)	1.2	1.2	1.2
Ramachandran plot			
Most favored (%)	91.5	93.1	91.0
Additional allowed regions (%)	8.0	6.3	8.5
Generously allowed regions (%)	0.5	0.5	0.5

[a]Values in parentheses correspond to the highest-resolution shell.
[b]$R_{sym} = [\sum_h \sum_i |I_i(h) - \langle I(h)\rangle| / \sum_h \sum_i I_i(h)] \times 100$, where $\langle I(h)\rangle$ is the mean of the $I(h)$ observation of reflection i.
[c]$R = \sum_{hkl} |F_o - F_c| / \sum_{hkl} |F_o|$.
[d]R_{free} was calculated as R but using only data reserved for the cross-validation (percentage shown in parentheses).

functions in both the dimer interface and glutathione binding, and Asp101 binds glutathione across the dimer interface, providing a link between dimerization and catalysis. The carboxylate group of the γ-glutamyl region forms hydrogen bonds with both the main-chain and side-chain of Ser68. Although most interactions between Sj26GST and the glutathione moiety of the ligands are hydrogen bonds, there are van der Waals interactions between the γ-glutamyl and side-chains of Leu13, Asn54, and Gln67, as well as between the cysteinyl moiety and Trp8.

In addition, there are water-mediated interactions between Sj26GST and the γ-glutamyl region of the glutathione moiety of the ligands. The main-chain of the *cis* Pro56 and Gln67 form water-mediated hydrogen bonds to the glutamyl carboxylate through one water molecule, while the main-chain of Met69 and side-chain of Gln67 use a second water molecule. The only structure where these water-mediated interactions are not observed is the Sj26GSTIBZ complex, which is likely due to its lower resolution (2.6 Å).

The conformation of GSH in these three complexes differs slightly from that observed with Sj26GST fused with a GP41 peptide and bound to glutathione.[16] The glycyl ϕ differs by approximately 90°, resulting in a significant difference in the position of the glycyl amino group. Similarly, a rotation of 25° around ϕ and 102° around χ_1 in the cysteinyl region place the side-chain in a slightly different position. Finally, a 46° rotation of ψ and χ_1 and a 78° rotation of χ_2 result in a small displacement of the Cα and Cβ of the glutamyl region.

Electrophile Binding Site (H Site)

Interactions of the Sj26GST H site are apparent from the binding mode of Sj26GST to S-hexyl, S-2-iodobenzyl, and sulfate moieties of our three glutathione product analogs. The only H site interactions introduced by the glutathione sulfonate of Sj26GSTSLF are with Tyr7, which forms direct and water-mediated hydrogen bonds with the sulfonate moiety [Fig. 1(A)]. In contrast, the S-hexyl and S-2-iodobenzyl moieties sit in a pocket lined with the side-chains of three distinct structural elements: the β1-α1 loop (Tyr7, Ile10, Gly12, Leu13), the end of the central α4 helix (Arg103, Tyr104, Ser107, Tyr111), and the C-

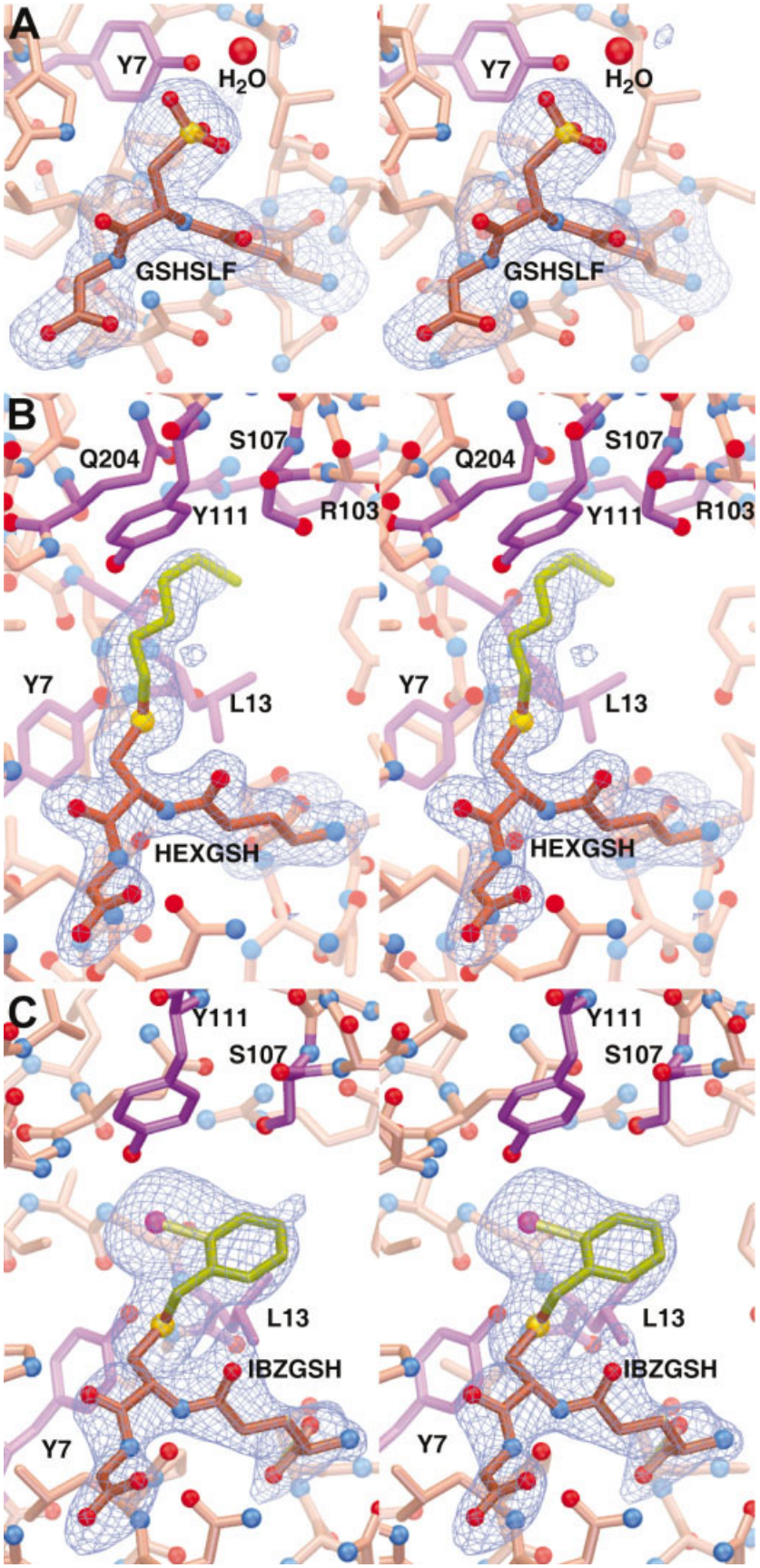

Fig. 1. Binding of product analogs to the H and G sites of Sj26GST. σA-weighted *Fo* − *Fc* electron density, contoured at 3.0σ, is shown for the ligands (glutathione in brown, S-hexyl and S-2-iodobenzyl in yellow). Functionally important H site residues are shown in purple. (**A**) Glutathione sulfonate. Tyr7 and a water molecule participate in a hydrogen bond with the sulfonate. (**B**) S-hexyl glutathione. Tyr7, Gly12, Leu13, Arg103, Ser107, Tyr111, and Gln204 participate in the S-hexyl moiety binding to the H site. (**C**) S-2-Iodobenzyl glutathione. Tyr7, Leu13, Ser107, and Tyr111 participate in binding the 2-iodobenzyl moiety at the H site.

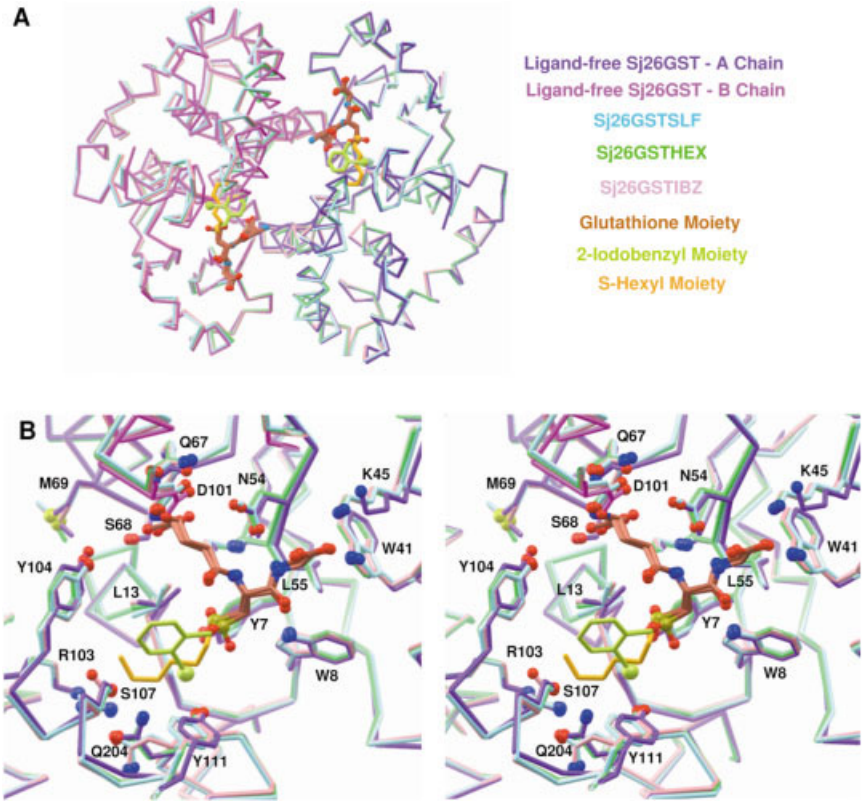

Fig. 2. Superposition of the Sj26GSTSLF, Sj26GSTHEX, and Sj26GSTIBZ complexes onto ligand-free Sj26GST structure. (**A**) Overall superposition of monomer A of the ligand-bound Sj26GSTs and ligand-free Sj26GST. The Cα traces of the superimposed monomers of Sj26GSTSLF (light blue), Sj26GSTHEX (light green), and Sj26GSTIBZ (light pink) complexes with ligand-free Sj26GST (purple) are nearly identical, indicating little change in the monomeric structure upon ligand binding. However, the nonsuperimposed subunit of ligand-free Sj26GST (magenta) lies closer to its aligned subunit than the unaligned subunits of the complexes, indicating an opening of the dimer interface to accommodate the ligands (glutathione in brown, S-hexyl in yellow, and S-2-iodobenzyl in orange). (**B**) Side-chain rotations of Ser107 in the Sj26GSTHEX complex and Gln204 in the Sj26GSTHEX and Sj26GSTIBZ complexes also occur to accommodate the hexyl and S-2-iodobenzyl moieties in the H site of Sj26GST.

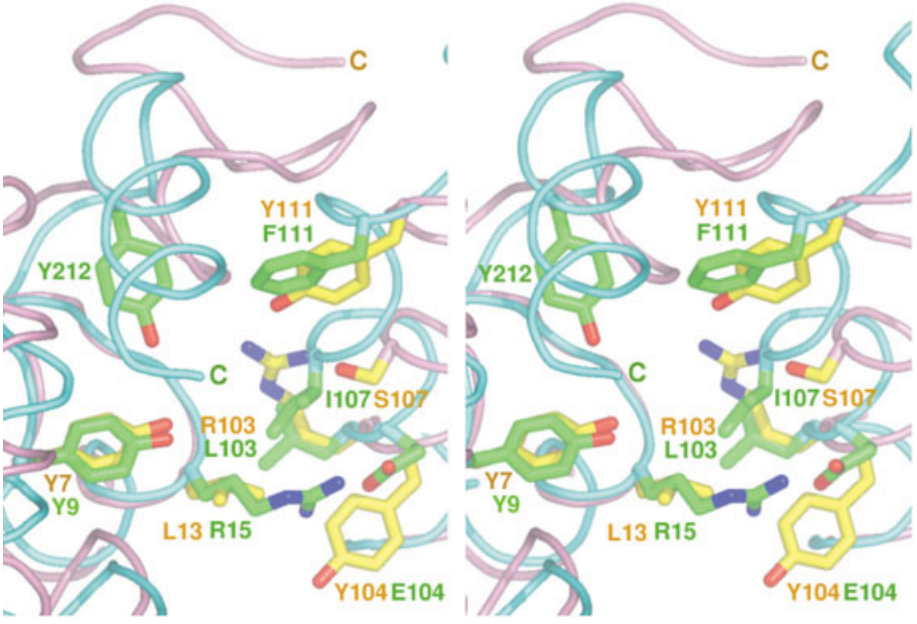

Fig. 3. Superposition of the Sj26GST and hGST A4-4 H sites. Functionally important H site residues of Sj26GST (pink trace and yellow side-chains) and hGST A4-4 (blue trace pink and green side-chains) are shown. The C-terminal coil of Sj26GST adopts an α-helical structure in A4-4.

TABLE II. Docking Results of Sj26GST–Substrate Complexes

Substrate	Rank	Conformations per cluster	Lowest (mean) free energy (kcal/mol)	Cluster RMSD (Å)
4HNE	1	60	−7.10 (−7.54)	1.27 ± 0.58
	2	60	−7.46 (−7.95)	1.16 ± 0.69
	3	52	−7.17 (−7.67)	1.34 ± 0.50
	4	12	−6.97 (−7.44)	1.38 ± 0.59
	5	11	−7.23 (−7.96)	1.16 ± 0.60
NE	1	96	−6.92 (−7.17)	0.68 ± 0.22
	2	60	−7.11 (−7.34)	0.71 ± 0.36
	3	59	−6.76 (−6.98)	0.83 ± 0.34
	4	41	−6.92 (−7.04)	0.89 ± 0.40
EA	1	203	−8.83 (−9.04)	0.50 ± 0.55
	2	33	−7.94 (−8.06)	0.31 ± 0.24
	3	9	−7.60 (−7.74)	0.20 ± 0.10
	4	5	−7.02 (−7.12)	0.92 ± 0.57
	5	4	−7.64 (−7.72)	0.32 ± 0.22

terminal coil (Gln204, Gly205) [Figs. 1(B), 1(C), and 2(B)]. The S-2-iodobenzyl substituent lies in a hydrophobic crevice defined by Leu13, Tyr104, Ser107, Tyr111, and Gln204 [Figs. 1(C) and 2(B)]. The benzyl ring stacks between the side-chains of Tyr104 and Tyr111 and has van der Waals interactions with Leu13. The iodine atom of S-2-iodobenzyl glutathione has polar interactions with the hydroxyl group of Tyr7 and Tyr111. The S-hexyl substituent in the Sj26GSTHEX complex nestles in a crevice defined by Ile10, Gly12, Leu13, Arg103, Tyr104, Ser107, Gln204, and Gly205 [Figs. 1(B) and 2(B)]. Due to structural similarity between S-hexyl glutathione and the conjugation product of glutathione and 4HNE, this orientation is likely representative of the 4HNE binding mode.

Inspection of the H sites of the superimposed Sj26GSTHEX, Sj26GSTSLF, Sj26GSTIBZ, and ligand-free Sj26GST structures reveals differences in the conformation of some H site residues [Fig. 2(B)]. There is a rotation of ≈120° about the χ_1 of Ser107 in the Sj26GSTHEX complex compared to the other two ligand-bound and the ligand-free Sj26GST structures. This change is necessary to avoid steric collision between O_γ of Ser107 and the hexyl moiety of the ligand. In addition, Gln204 has a rotation of ≈30° about the χ_1 in Sj26GSTHEX and Sj26GSTIBZ complexes compared to the ligand-free Sj26GST structures, accommodating the extra hexyl and 2-iodobenzyl moieties in the H site of Sj26GST. Therefore, changes in the Ser107 and Gln204 dihedral angles make the H site of Sj26GST more hydrophobic.

Comparison to Mammalian GST Binding Sites

The glutathione binding site of Sj26GST shares most features with the mammalian mu class GST structures.[7,16] The largest difference between the G sites of Sj26GST and other mu GSTs are substitutions in three G site residues: Met69 (Asn in human and rat GSTs M1-1 and M2-2), Gly97 (Asn in human and rat GSTs M1-1 and M2-2), and Tyr104 (Met in human GSTs M1-1 and M2-2 and rat GST M1-1; Leu in rat GST M2-2). Interactions of these residues were unchanged, however, as they all make water-mediated hydrogen bonds with the glutamyl moiety of glutathione in Sj26GST.

Although the G sites of Sj26GST and mammalian mu GSTs are structurally similar, their H sites differ significantly. The largest difference is an eight-residue insertion in a loop of the mammalian mu GST that walls off one side of the H site. The replacement of this loop by a β-turn in Sj26GST (between residues 34 and 38) increases the solvent exposure of this region of the H site. In contrast, aromatic residues (Trp206 and Tyr104) partially block entrances to the Sj26GST H site as compared to the human mu GST.

Despite the fact that Sj26GST is most structurally similar to the mu class, its H site bears a higher similarity to that of human alpha GST A4-4 (hGST A4-4). The features of these binding pockets confer specificity of both proteins toward alkenals.[7,14] Mutational analysis of hGST A4-4 Tyr212 supports the hypothesis that this residue is important for specificity toward 4HNE.[7] The important role of hGST A4-4 Tyr212 in substrate polarization seems to be accomplished by Sj26GST Tyr111 (Fig. 3). In addition, Gly12 is conserved in both proteins because any other residue would prevent Tyr111 (or Tyr212 in hGST A4-4) from occupying its position. This assumption is supported by mutagenesis results for rat GST A4-4 demonstrating that Gly12 is necessary for the high catalytic efficiency and specificity of GST A4-4 toward 4HNE.[7] In addition, there is a compensatory pair of mutations between the H sites of Sj26GST and hGST A4-4: Leu13 in Sj26GST corresponds to Arg15 in hGST A4-4 and its neighbor Arg103 in Sj26GST to Leu103 in hGST A4-4. This compensatory pair of mutations keeps intact the chemistry of the H site associated with these two neighboring residues. The largest differences between the H sites of Sj26GST and hGST A4-4 occur in the C-terminal region. While the C-terminus of Sj26GST folds as a coil and seems to act as a flexible "cap" for the H site in a similar way as in mammalian mu class GSTs, in hGST A4-4 it folds as an extra α-helix and participates in the binding of both glutathione and electrophile[7] (Fig. 3). There are also substitutions of Sj26GST Tyr104, Ser107, and Arg108 with Glu104, Ile107, and Met108 in hGST A4-4, respectively.

Proposed Binding Mode of Physiologic Substrates

Sj26GST exhibits glutathione conjugation activity toward alkenals, established secondary products of membrane lipid peroxidation, and ethacrynic acid.[14] The major 4-hydroxyalkenal formed during peroxidation of arachidonic and linoleic acids, 4HNE, is highly cytotoxic and mutagenic. Ethacrynic acid enhances excretion of sodium, chloride, and potassium and produces diuretic effects. Sj26GST catalyzes the addition of GSH to the alkene of these compounds to facilitate their removal.

Analysis of the H site identifies key features that permit the construction of a model for the binding of 4HNE to Sj26GST. The structure of Sj26GST bound to S-hexyl glutathione delineates the hydrophobic binding pocket for the aliphatic groups beyond carbon 3, the target of glutathione addition, but does not indicate the binding mode of the aldehydic and hydroxyl moieties. To model these and other interactions, we performed computational docking of Sj26GST with its physiologic substrates 4HNE, NE, and EA. As a test

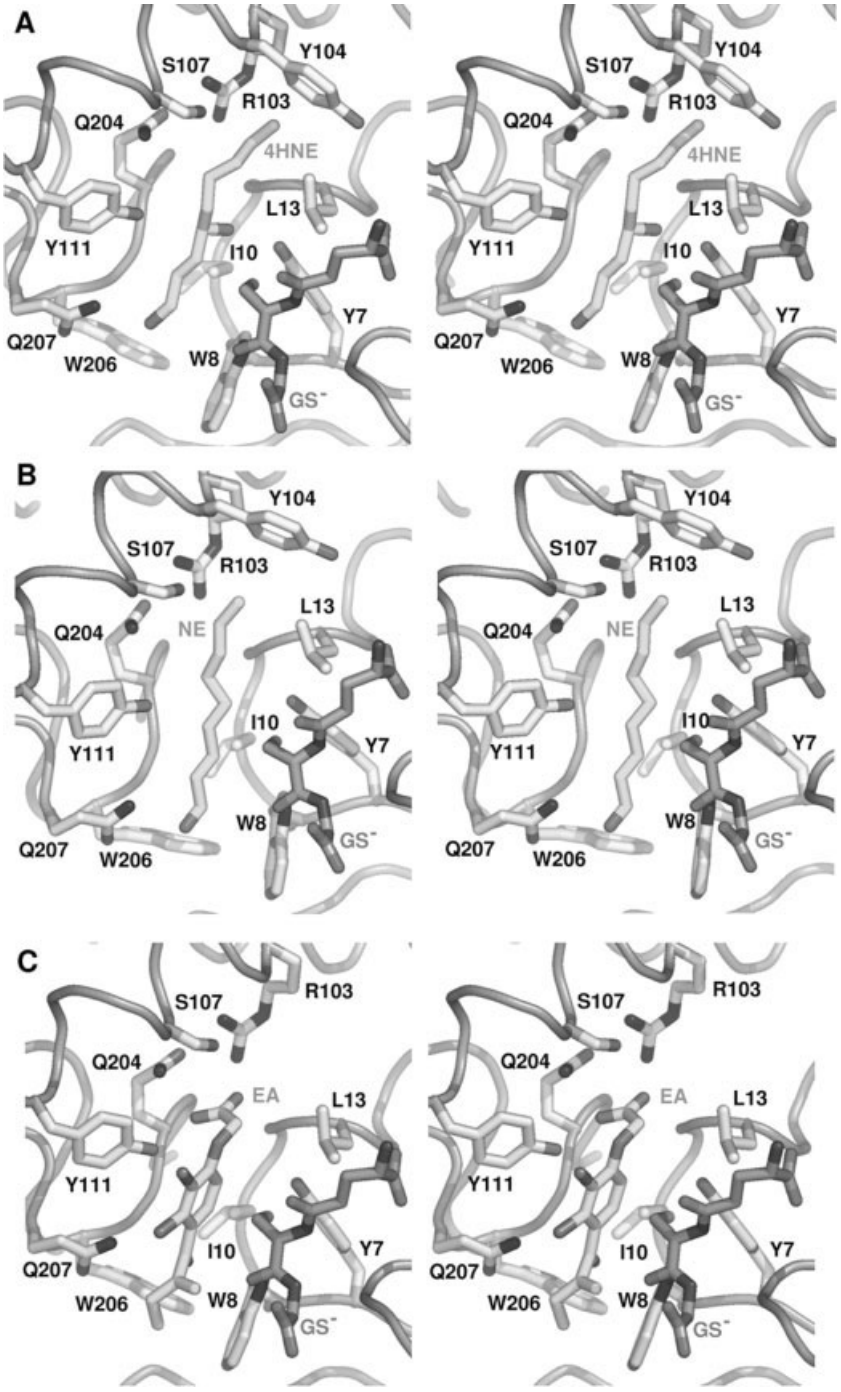

Fig. 4. Stereoview of the computationally predicted binding mode of Sj26GST to its physiological substrates (**A**) 4HNE, (**B**) NE, and (**C**) EA.

of the method, glutathione sulfonate, S-hexyl glutathione, and S-2-iodobenzyl glutathione were docked with an edited, ligand-free GST structure (see Methods section) and compared to the crystallographic complexes. The computationally predicted complexes are in good agreement with the crystallographic structures (the RMS deviation value for top conformers is 0.3 Å for Sj26GSTSLF, 1.6 Å for Sj26GSTHEX, and 3.1 Å for Sj26GSTIBZ), suggesting that this docking method may be used to predict the binding orientation of ligands to the G and H sites.

The top-scoring dockings of NE, 4HNE, and EA, with their free energy of binding and number of conformations per cluster, are shown in Table II. As the empirically determined standard error of AutoDock is approximately 2 kcal/mol,[33] the free energies of the top-scoring clusters for each ligand are not significantly different. The number of conformations in a cluster is therefore a more appropriate criterion by which to rank the dockings. Consistent with this ranking, the most populated clusters of NE and EA place the alkene within reactive proximity of the gluta-

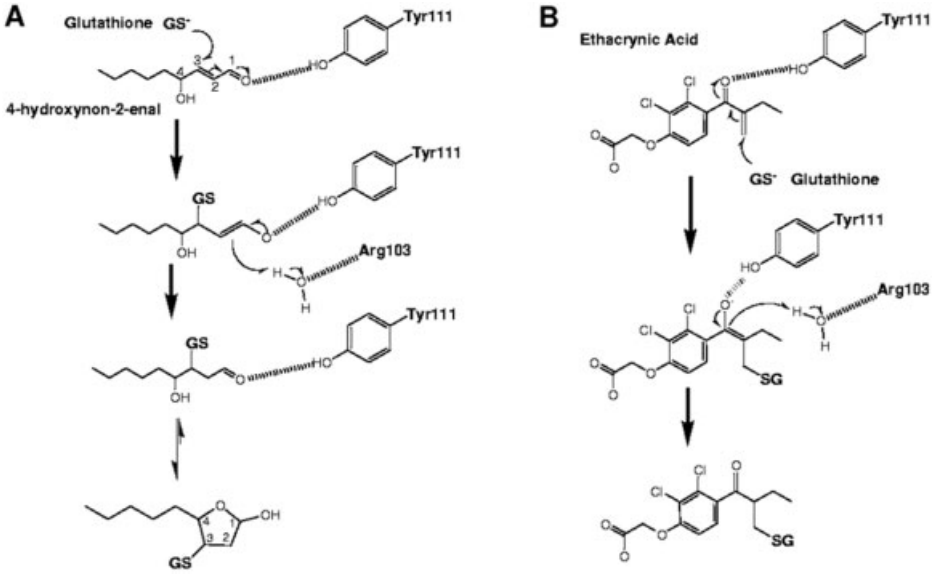

Fig. 5. Possible general mechanism of glutathione conjugation for (**A**) 4-hydroxynon-2-enal and (**B**) ethacrynic acid by Sj26GST. Tyr111 may activate the substrate by polarizing the aldehydic oxygen. Following addition of glutathione, the α carbon may be protonated by a water molecule activated by Arg103 or by Arg103 directly.

thione thiol. The docking of 4HNE results in two equally populated top clusters, but only one of these clusters appears similarly productive.

The general docking orientation of NE and 4HNE to Sj26GST is the same. The alkyl region of both ligands binds in the H site [Figs. 4(A) and 4(B)], similar to the structure of the Sj26GSTHEX complex [Figs. 1(B) and 2(B)]. The ligand alkyl chains interact with the side-chains of Trp8, Ile10, Gly12, Leu13, Arg103, Tyr104, Ser107, Gln204, Gly205, and Trp206. The hydroxyl group of 4HNE participates in hydrogen bonds with the side-chain of Tyr7 and main-chain of Leu13 [Fig. 4(A)], which may explain the higher specific activity of 4HNE to Sj26GST compared to NE.[14] Another important feature of the predicted 4HNE and NE binding modes is that Gln207 and Tyr111 make close contacts (3.0 and 5.7 Å, respectively) with the aldehydic oxygen of 4HNE and NE. This close contact may allow Tyr111 and/or Gln207 to both orient the substrate for conjugation and activate it by polarizing the aldehydic oxygen [Fig. 5(A)]. Carbon 2 of 4HNE and NE is also positioned appropriately to be protonated by a water molecule activated by Arg103 or by Arg103 itself [Fig. 5(A)].[7] Finally, the alkene moieties of both NE and 4HNE lie close to the thiolate anion (3.5 and 3.2 Å, respectively) of GSH and hydroxyl group of Tyr111, consistent with the docking representing a productive binding mode of the substrates.

The α,β-unsaturated ketone moiety of EA is also thought to conjugate with glutathione via Michael addition, both spontaneously and by GST-driven catalysis.[36] Computational docking predicts that EA binds in a pocket lined with the side-chains of Tyr7, Trp8, Ile10, Gly12, Leu13, Arg103, Ser107, Tyr111, Gln204, Gly205, Trp 206, and Gln207 [Fig. 4(C)]. In this complex, the carboxylate moiety of EA forms hydrogen bonds with the side-chains of Arg103 and Tyr111 and lies close to Ser107 and Gln204. The ether moiety of EA also accepts a hydrogen bond from the side-chain of Tyr111. One chlorine atom contacts the side-chain of Gln204 while the other points out to solution. The aromatic ring of EA packs between the side-chains of Trp8 and Tyr111 in an almost parallel stacking interaction. The EA ketone and butyryl moieties pack against Trp8, Ile10, Gly205, and Trp206. In Sj26GST, the electrophilicity of EA carbon 12 can be enhanced by the hydrogen bonding of Tyr111 and Gln207 to the EA ketone oxygen [Fig. 5(B)] in the same way as was suggested for the human pi class GST in complex with EA.[36] Although carbon 12, the target of nucleophilic attack, is 4.8 Å from the thiolate anion of glutathione in the lowest-energy docked complex of Sj26GST-EA, minimal motion of the inhibitor and protein could readily decrease this distance and promote the reaction.

CONCLUSIONS

The analysis of the crystallographic Sj26GSTSLF, Sj26GSTHEX, and Sj26GSTIBZ complexes identifies key features of the H site that direct the binding of these ligands. Together, crystallographic and docking results allow the modeling of Sj26GST interactions with its physiologic substrates NE, 4HNE, and EA. The substrates sit in a pocket defined by side-chains from the β1-α1 loop (Tyr7, Trp8, Ile10, Gly12, Leu13), helix α4 (Arg103, Tyr104, Ser107, Tyr111), and the C-terminal coil (Gln204, Gly205, Trp206, Gln207). Hydrogen bonding of Tyr111 and Gln207 to the aldehydic oxygen of 4HNE and NE and the ketone oxygen of EA could enhance their electrophilicity toward conjugate addition. These results provide insight into ligand binding by Sj26GST, an attractive drug target for structure-based design of adjuvants to praziquantel in schistosomiasis treatments.

Coordinates

The coordinates for Sj26GSTSLF, Sj26GSTHEX, and Sj26GSTIBZ complexes have been deposited in the PDB

(respective IDs 1M99, 1M9A, and 1M9B), to be released at the time of publication.

ACKNOWLEDGMENTS

The authors thank Ilona Canestrelli and Susan Bernstein for excellent technical support and assistance in the expression and purification of Sj26GST, Jesus M. Castagnetto and Victoria A. Roberts for valuable advice in docking analysis, and Arthur J. Olson and Garrett M. Morris for providing AutoDock 3.05 and useful suggestions. This work was supported by a grant from the National Institutes of Health (GM39345-13). R.M.F.C. gratefully acknowledges the scholarship from the Conselho Nacional de Desenvolvimento Científico e Tecnológico.

REFERENCE

1. Hayes JD, Pulford DJ. The glutathione S-transferase supergene family: regulation of GST and the contribution of the isoenzymes to cancer chemoprotection and drug resistance. Crit Rev Biochem Mol Biol 1995;30:445–600.
2. Wilce MC, Parker MW. Structure and function of glutathione S-transferases. Biochim Biophys Acta 1994;1205:1–18.
3. Board PG, Coggan M, Chelvanayagam G, Easteal S, Jermiin LS, Schulte GK, Danley DE, Hoth LR, Griffor MC, Kamath AV, Rosner MH, Chrunyk BA, Perregaux DE, Gabel CA, Geoghegan KF, Pandit J. Identification, characterization, and crystal structure of the omega class glutathione transferases. J Biol Chem 2000;275:24798–24806.
4. Sinning I, Kleywegt GJ, Cowan SW, Reinemer P, Dirr HW, Huber R, Gilliland GL, Armstrong RN, Ji X, Board PG,et al. Structure determination and refinement of human alpha class glutathione transferase A1-1, and a comparison with the mu and pi class enzymes. J Mol Biol 1993;232:192–212.
5. Ji X, Zhang P, Armstrong RN, Gilliland GL. The three-dimensional structure of a glutathione S-transferase from the mu gene class. Structural analysis of the binary complex of isoenzyme 3-3 and glutathione at 2.2-Å resolution. Biochemistry 1992;31:10169–10184.
6. Raghunathan S, Chandross RJ, Kretsinger RH, Allison TJ, Penington CJ, Rule GS. Crystal structure of human class mu glutathione transferase GSTM2-2. Effects of lattice packing on conformational heterogeneity. J Mol Biol 1994;238:815–832.
7. Bruns CM, Hubatsch I, Ridderstrom M, Mannervik B, Tainer JA. Human glutathione transferase A4-4 crystal structures and mutagenesis reveal the basis of high catalytic efficiency with toxic lipid peroxidation products. J Mol Biol 1999;288:427–439.
8. Reinemer P, Dirr HW, Ladenstein R, Schaffer J, Gallay O, Huber R. The three-dimensional structure of class pi glutathione S-transferase in complex with glutathione sulfonate at 2.3 Å resolution. EMBO J 1991;10:1997–2005.
9. Wilce MC, Board PG, Feil SC, Parker MW. Crystal structure of a theta-class glutathione transferase. EMBO J 1995;14:2133–2143.
10. Ji X, von Rosenvinge EC, Johnson WW, Tomarev SI, Piatigorsky J, Armstrong RN, Gilliland GL. Three-dimensional structure, catalytic properties, and evolution of a sigma class glutathione transferase from squid, a progenitor of the lens S-crystalline of cephalopods. Biochemistry 1995;34:5317–5328.
11. Thom R, Dixon DP, Edwards R, Cole DJ, Lapthorn AJ. The structure of a zeta class glutathione S-transferase from *Arabidopsis thaliana*: characterisation of a GST with novel active-site architecture and a putative role in tyrosine catabolism. J Mol Biol 2001;308:949–962.
12. Dirr H, Reinemer P, Huber R. X-ray crystal structures of cytosolic glutathione S-transferases. Implications for protein architecture, substrate recognition and catalytic function. Eur J Biochem 1994;220:645–661.
13. Brophy PM, Barrett J. Glutathione transferase in helminths. Parasitology 1990;100(2):345–349.
14. Walker J, Crowley P, Moreman AD, Barrett J. Biochemical properties of cloned glutathione S-transferases from *Schistosoma mansoni* and *Schistosoma japonicum*. Mol Biochem Parasitol 1993;61:255–264.
15. McTigue MA, Williams DR, Tainer JA. Crystal structures of a schistosomal drug and vaccine target: glutathione S-transferase from *Schistosoma japonica* and its complex with the leading antischistosomal drug praziquantel. J Mol Biol 1995;246:21–27.
16. Lim K, Ho JX, Keeling K, Gilliland GL, Ji X, Ruker F, Carter DC. Three-dimensional structure of *Schistosoma japonicum* glutathione S-transferase fused with a six-amino acid conserved neutralizing epitope of gp41 from HIV. Protein Sci 1994;3:2233–2244.
17. Capron A, Capron M, Dombrowicz D, Riveau G. Vaccine strategies against schistosomiasis: from concepts to clinical trials. Int Arch Allergy Immunol 2001;124:9–15.
18. Grzych JM, De Bont J, Liu J, Neyrinck JL, Fontaine J, Vercruysse J, Capron A. Relationship of impairment of schistosome 28-kilodalton glutathione S-transferase (GST) activity to expression of immunity to *Schistosoma mattheei* in calves vaccinated with recombinant *Schistosoma bovis* 28-kilodalton GST. Infect Immunol 1998;66:1142–1148.
19. Hassanein H, Kamel M, Badawy A, El-Ghorab N, Abdeen H, Zada S, El-Ahwany E, Doughty B. Anti-miracidial effect of recombinant glutathione S-transferase 26 and soluble egg antigen on immune responses in murine *Schistosomiasis mansoni*. APMIS 1999;107:723–736.
20. Botros SS, Makary EA, Ahmed KM, Ibrahim AM, Nashed NN, El-Nahal HM, Doughty BL, Hassanein HI. Effect of combined praziquantel and recombinant glutathione S-transferase on resistance to reinfection in murine *Schistosomiasis mansoni*. Int J Immunopharmacol 2000;22:979–988.
21. Xiao B, Singh SP, Nanduri B, Awasthi YC, Zimniak P, Ji X. Crystal structure of a murine glutathione S-transferase in complex with a glutathione conjugate of 4-hydroxynon-2-enal in one subunit and glutathione in the other: evidence of signaling across the dimer interface. Biochemistry 1999;38:11887–11894.
22. Srivastava S, Chandra A, Wang LF, Seifert WE Jr, DaGue BB, Ansari NH, Srivastava SK, Bhatnagar A. Metabolism of the lipid peroxidation product, 4-hydroxy-trans-2-nonenal, in isolated perfused rat heart. J Biol Chem 1998;273:10893–10900.
23. Lauwers L. Clinical experience with a new diuretic: ethacrinic acid. Acta Cardiol 1966;21:79–89.
24. McTigue MA, Bernstein SL, Williams DR, Tainer JA. Purification and crystallization of a schistosomal glutathione S-transferase. Proteins 1995;22:55–57.
25. Otwinowski Z, Minor W. Processing of x-ray diffraction data collected in oscillation mode. Meth Enzymol 1997;276:307–326.
26. Collaborative Computational Project Number 4. The CCP4 Suite: programs for protein crystallography. Acta Crystallogr 1994;D50: 760–763.
27. Navaza J. AMoRe: An automated package for molecular replacement. Acta Crystallogr 1994;A50:157–163.
28. Tronrud DE. TNT refinement package. Meth Enzymol 1997;277: 306–319.
29. Brunger AT, Adams PD, Clore GM, DeLano WL, Gross P, Grosse-Kunstleve RW, Jiang J-S, Kuszewski J, Nilges N, Pannu NS, Read RJ, Rice LM, Simonson T, Warren GL. Crystallography and NMR system (CNS): A new software system for macromolecular structure determination. Acta Crystallogr. 1998;D54:905–921.
30. McRee DE. XtalView/Xfit—A versatile program for manipulating atomic coordinates and electron density. J Struct Biol 1999;125: 156–165.
31. Laskowski RA, MacArthur MW, Moss DS, Thornton JM. PROCHECK: a program to check the stereochemical quality of protein structures. J Appl Crystallogr 1993;26:283–291.
32. McDonald IK, Thornton JM. Satisfying hydrogen bonding potential in proteins. J Mol Biol 1994;238:777–793.
33. Morris GM, Goodsell DS, Halliday RS, Huey R, Hart WE, Belew RK, Olson A. Automated docking using a Lamarckian genetic algorithm and empirical binding free energy function. J Comput Chem 1998;19:1639–1662.
34. Weiner SJ, Kollman PA, Case DA, Singh UC, Ghio C, Alagona G, Profeta SJ,Weiner P. A new force field for molecular mechanical simulation of nucleic acids and proteins. J Am Chem Soc 1984;106: 765–784.
35. Dauber-Osguthorpe P, Roberts VA, Osguthorpe DJ, Wolff J, Genest M, Hagler AT. Structure and energetics of ligand binding to proteins: *E. coli* dihydrofolate reductase-trimethoprim, a drug–receptor system. Proteins 1988;4:31–47.
36. Oakley AJ, Rossjohn J, Lo Bello M, Caccuri AM, Federici G, Parker MW. The three-dimensional structure of the human pi class glutathione transferase P1-1 in complex with the inhibitor ethacrynic acid and its glutathione conjugate. Biochemistry 1997; 36:576–585.